Electron-phonon superconductivity near charge-density-wave instability in $LaO_{0.5}F_{0.5}BiS_2$: Density-functional calculations

Xiangang Wan,[1,2] Hang-Chen Ding,[3] Sergey Y. Savrasov,[2] and Chun-Gang Duan[3,4]

[1]*National Laboratory of Solid State Microstructures and Department of Physics, Nanjing University, Nanjing 210093, China*

[2]*Department of Physics, University of California, Davis, One Shields Avenue, Davis, California 95616, USA*

[3]*Key Laboratory of Polar Materials and Devices, Ministry of Education, East China Normal University, Shanghai 200062, China*

[4]*National Laboratory for Infrared Physics, Chinese Academy of Sciences, Shanghai 200083, China*

(Received 8 August 2012; revised manuscript received 7 March 2013; published 18 March 2013)

We discuss the electronic structure, lattice dynamics, and electron-phonon interaction of the newly discovered superconductor $LaO_{0.5}F_{0.5}BiS_2$ using density-functional-based calculations. A strong Fermi surface nesting at $\mathbf{k} = (\pi,\pi,0)$ suggests a proximity to charge-density-wave instability and leads to imaginary harmonic phonons at this $\mathbf{k}$ point associated with in-plane displacements of S atoms. Total energy analysis resolves only a shallow double-well potential well preventing the appearance of static long-range order. Both harmonic and anharmonic contributions to electron-phonon coupling are evaluated and give a total coupling constant $\lambda \simeq 0.85$, prompting this material to be a conventional superconductor contrary to structurally similar FeAs materials.

DOI: 10.1103/PhysRevB.87.115124 PACS number(s): 74.20.Pq, 74.25.Jb, 74.25.Kc, 74.70.−b

I. INTRODUCTION

Superconductors with layered crystal structures such as cuprates,[1] ruthenates,[2] or MgB_2 (Ref. 3) have generated enormous research interest. A recent discovery of iron pnictides[4] triggered another wave of extensive studies,[5] and while the mediator of pairing in these systems remains officially unidentified, a large amount of evidence points to magnetic spin fluctuations induced by antiferromagnetic spin-density-wave (SDW) instability due to Fermi-surface nesting[6] at wave vector $\mathbf{k} = (\pi,\pi,0)$ similar to the cuprates. Usually changing the blocking layer can tune the superconducting T_c, thus searching for new layered superconductors is of both fundamental and technological importance.

Very recently, a new layered superconductor $Bi_4O_4S_3$ was found,[7] and soon after, two other systems, $LaO_{1-x}F_xBiS_2$ (Ref. 8) and $NdOBiS_2$ (Ref. 9), were discovered. Here, the basic structural unit is the BiS_2 layer which is similar to the Cu-O planes in Cu-based superconductors[1] and the Fe-A (A = P, As, Se, and Te) planes in iron pnictides.[5] A chance to explore superconductivity and increase T_c in these new compounds has already resulted in a lot of work that appeared shortly after the discovery.[7–16] Hall effect measurements reveal multiband features and suggest that superconducting pairing occurs in one-dimensional chains.[10] It was proposed that these compounds are type-II superconductors and good candidates for thermoelectric materials.[11] Electrical resistivity measurements under pressure reveal that $Bi_4O_4S_3$ and $La(O,F)BiS_2$ have different T_c versus pressure behavior, and the Fermi surface of $La(O,F)BiS_2$ may be located in the vicinity of some instabilities.[12] A two p bands electronic model has been proposed based on band-structure calculation,[13] and a good Fermi-surface nesting with wave vector $\mathbf{k} = (\pi,\pi,0)$ has been found.[13] The importance of the nesting has been emphasized experimentally[12] and it was suggested that electronic correlations may play a role in the superconductivity of these systems.[14]

Here we report our theoretical studies of the electronic structure and lattice dynamic properties for $LaO_{0.5}F_{0.5}BiS_2$, the compound that possesses the highest $T_c \simeq 10$ K (Ref. 8) among known BiS-based materials[7–9] and whose structure is similar to superconducting iron arsenides $LaFeO_{1-x}F_xAs$.[4] Our first-principles calculations are based on density-functional theory (DFT) and show that the bands around the Fermi level are not sensitive to F substitution, thus making the rigid band approximation adequate for $LaO_{1-x}F_xBiS_2$. We find a strong nesting of the Fermi surface at $\mathbf{k} = (\pi,\pi,0)$ for $x = 0.5$ by performing the calculation for ordered compound $LaO_{0.5}F_{0.5}BiS_2$. Our linear-response-based phonon calculation shows that the nesting results in a large phonon softening at this $\mathbf{k}$ and in the appearance of the imaginary modes associated with in-plane displacements of S atoms. Our $\sqrt{2} \times \sqrt{2} \times 1$supercell total-energy calculation finds a shallow double-well potential prompting that these displacements are dynamic. Contrary to the expectations that electronic correlations may play a role in these systems, our calculated electron-phonon coupling constant $\lambda \simeq 0.85$ suggests that this material is a conventional superconductor. However, our anharmonic model calculation shows that the vicinity of the charge-density-wave (CDW) instability is essential for the superconductivity, which is reminiscent of iron pnictides whose proximity to SDW is well established.[4]

II. COMPUTATION METHOD

Our electronic structure calculations are performed within the generalized gradient approximation (GGA).[17] Whenever possible, we cross-check the results using two different commonly used total-energy codes: (a) the Vienna Ab-Initio Simulation Package (VASP)[18] and (b) the QUANTUM ESPRESSO package (QE).[19] The consistency of our results for two sets of calculations is satisfactory. We use a 500 eV plane-wave cutoff and a dense $18 \times 18 \times 6$ k-point mesh in the irreducible Brillouin zone (IBZ) for self-consistent calculations. For structural optimization, the positions of the ions were relaxed toward equilibrium until the Hellmann-Feynman forces became less than 2 meV/Å. For the phonon calculations, we adopted a scalar relativistic version of the density-functional linear-response method[20] as implemented in QE.[19] For consistency,

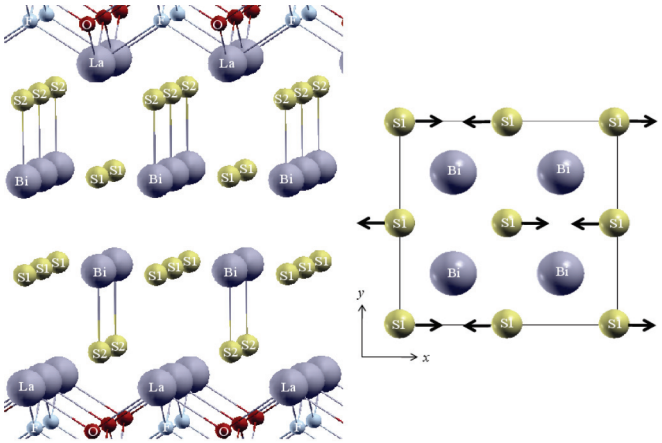

(a) (b)

FIG. 1. (Color online) (a) Structure of $La(O_{0.5}F_{0.5})BiS_2$; (b) unstable phonon mode corresponding to wave vector $\mathbf{k} = (\pi,\pi,0)$.

the results presented in this paper were obtained by a scalar relativistic version of QE, unless otherwise specified. The effect of spin-orbit coupling (SOC) is also discussed.

III. RESULTS AND DISCUSSIONS

The powder x-ray diffraction (XRD) pattern shows that $LaO_{1-x}F_xBiS_2$ forms a layered crystal structure with a space group $P4/nmm$.[8] La, S, and Bi are located at the $2b$ position, while O/F take the $2a$ site. Similar to $LaO_{1-x}F_xFeAs$,[4] the structure consists of alternating $La(O_{1-x}F_x)$ and BiS_2 layers.[8] One BiS_2 layer contains two BiS planes (namely the Bi-S1 plane) and two pure S planes (i.e., the S2 plane), as shown in Fig. 1(a). To study the influence of F doping, we carried out calculations for two systems, i.e., $LaOBiS_2$ ($x = 0$) and $LaO_{0.5}F_{0.5}BiS_2$ ($x = 0.5$). Being that it is embedded into the LaO plane, we expect that the substitution by F has only a small effect on the BiS_2 layer. Thus we simulate $LaO_{0.5}F_{0.5}BiS_2$ by replacing half of the oxygen $2a$ sites by F orderly, even though the substitution may be random in reality. The optimized lattice parameters and Wyckoff positions for each atom are shown in Table I, together with available experimental data.[8] While the overall agreement between numerical and experimental structures is good, Table I reveals an interesting aspect: the differences between the experimental and theoretical values of the z coordinate of S1 are unusually large, as in the FeAs superconductors.[21] There is also a large difference between the numerical and experimental interlayer distances. Note that we have also performed the internal atomic coordinates optimization based on the experimental lattice parameters, as shown in Table II. As can be seen from Table II, the lattice parameters, i.e., the interlayer distances, have only a small effect on the z coordinate of S1. In Table I we also list the numerical data for $LaOBiS_2$. Comparing with the results for $LaO_{0.5}Bi_{0.5}S_2$, one can conclude that F substitution has only a small effect on the lattice parameters and a small effect on the BiS_2 layer.

TABLE I. Calculated lattice parameters and Wyckoff positions of $LaOBiS_2$ and $La(O_{0.5}F_{0.5})BiS_2$. Experimental results[8] are also listed for comparison.

		$LaOBiS_2$		$La(O_{0.5}F_{0.5})BiS_2$	
	Site	Calc.	Expt.	Calc.	Expt.
a (Å)		4.0394		4.0780	4.0527
c (Å)		14.1232		13.4925	13.3237
z	La ($2b$)	0.0889		0.1049	0.1015
z	Bi ($2b$)	0.6304		0.6141	0.6231
z	S1 ($2b$)	0.3932		0.3902	0.3657
z	S2 ($2b$)	0.8090		0.8134	0.8198
z	O ($2a$)	0.0000		0.0000	0.0000
z	F ($2a$)			0.0000	0.0000

TABLE II. The numerical Wyckoff positions of $La(O_{0.5}F_{0.5})BiS_2$ based on the experimental lattice parameter. Experimental Wyckoff positions[8] are also listed for comparison.

	$La(O_{0.5}F_{0.5})BiS_2$		
	Site	Calc.	Expt.
z	La ($2b$)	0.1064	0.1015
z	Bi ($2b$)	0.6149	0.6231
z	S1 ($2b$)	0.3838	0.3657
z	S2 ($2b$)	0.8137	0.8198
z	O ($2a$)	0.0000	0.0000
z	F ($2a$)	0.0000	0.0000

The discrepancy between the experimental and theoretical positions of S1 atoms results in a considerable difference for the valence band, as shown in Fig. 2(a). We also perform a calculation based on the numerical internal atomic coordinates and experimental lattice parameters. A comparison with the results based on theoretical structure shows that changing the interlayer distance only slightly affects the band structure, and the considerable difference shown in Fig. 2(a) is mainly due to the z coordinate of S1. For $LaOBiS_2$, both S $3p$ and O $2p$ states appear mainly between -4.0 and 0.0 eV. Although it is located primarily above the Fermi level, Bi $6p$ also makes a considerable contribution to the states between -4.0 and 0.0 eV, indicating a strong hybridization between Bi $6p$ and S

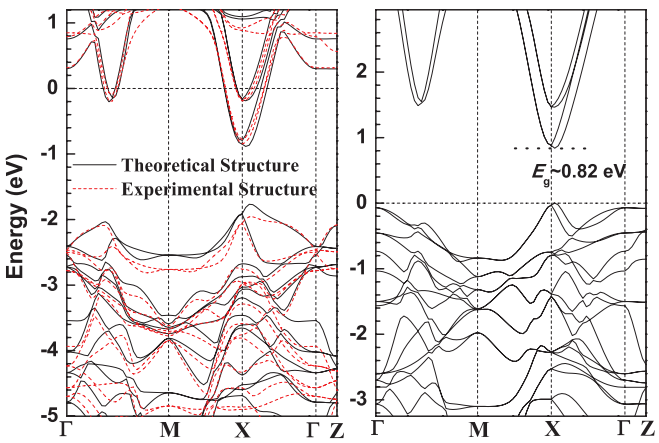

(a) (b)

FIG. 2. (Color online) Band structure of (a) $LaO_{0.5}F_{0.5}BiS_2$ and (b) $LaOBiS_2$.

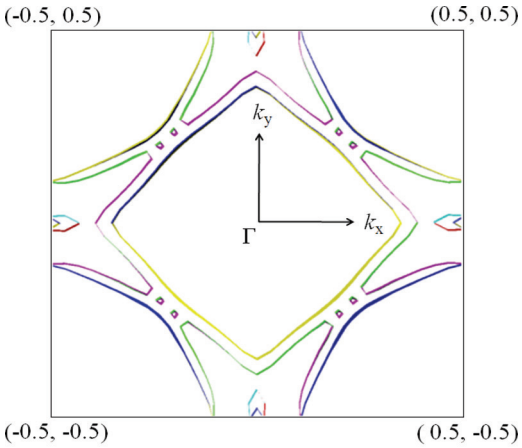

FIG. 3. (Color online) Calculated Fermi surface of $La(O_{0.5}F_{0.5})BiS_2$: (a) cross section for $k_z = 0$, (b) 3D view.

$3p$ states. In agreement with previous calculation,[13] our results show that $LaOBiS_2$ is an insulator with a band gap of 0.82 eV.A little dispersion along the Γ to the Z line clearly shows a two-dimensional character of the band structure, which indicates that the interlayer hybridization is small. Comparing Figs. 2(a) and 2(b), it is clear that the main influence of F substitution is a carrier doping characterized by the associated upshift of the Fermi level towards the Bi 6 p band, and the system becomes metallic as shown in Fig. 2(a). It is interesting to notice that doping by F has a negligible effect on the lowest conduction band. Thus we conclude that the rigid band approximation is valid for $LaO_{1-x}F_xBiS_2$.

There are four bands that cross the Fermi level and result in a large two-dimensional-like Fermi surface that is shown in Fig. 3. Consistent with the tight-binding result,[13] our density functional calculation shows a strong Fermi surface nesting at wave vectors near $\mathbf{k} = (\pi,\pi,0)$.

The Bi $6p$ orbitals are spatially extended and strongly hybridized with S $3p$ states near the Fermi energy. Thus we do not expect electronic correlations to be essential for this compound. To check whether the conventional electron-phonon mechanism can be responsible for superconductivity here, we first perform a linear-response phonon calculation[20] as implemented in QE.[19] An $18 \times 18 \times 6$ grid was used for the integration over IBZ. Our calculated phonon spectrum along major high-symmetry lines of the Brillouin zone is shown in

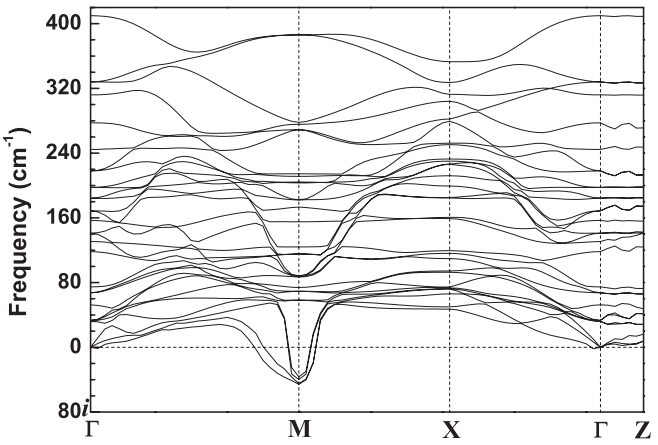

FIG. 4. Calculated phonon dispersions for $LaO_{0.5}F_{0.5}BiS_2$ using a density-functional linear-response approach.

Fig. 4 where the phonon dispersions are seen to extend up to 400 cm^{-1}. The phonon modes have only a little dispersion along the Γ-Z direction, which again indicates the smallness of the interlayer coupling. There are basically three panels in the phonon spectrum that are easily distinguished along the Γ-Z direction. The top four branches above 300 cm^{-1} are mainly contributed by O and F, while the branches below 80 cm^{-1} come from the BiS_2 layer. The phonon vibrations within the xy plane show a significant dispersion as shown in Fig. 4. Analyzing the evolution of the phonon eigenvectors in the Brillouin zone reveals that there is a clear separation between the xy- and z-polarized vibrations, and most of the modes show a definite in-plane or out-of-plane character.

A striking feature of this phonon spectrum is the presence of phonon softening around the M point that we associate with the strong Fermi surface nesting. We find that there are four totally unstable modes, mainly contributed by the S1 in-plane vibrations, where they either displace along the x or y direction, and they are either in-phase or out-of-phase between the two BiS planes. The polarization vectors are shown in Fig. 1(b).

To understand whether the CDW instability is present in this material, we perform a frozen phonon analysis with the unit cell doubled ($\sqrt{2} \times \sqrt{2} \times 1$) according to the $(\pi,\pi,0)$ nesting wave vector. We perform four calculations by moving the atoms according to the eigenvectors of the four unstable phonon modes at the M point. Our frozen phonon calculations show a shallow double-well potential where the S1 atoms shift about 0.18 Å away from the original high-symmetry position, as we show in Fig. 5. To illustrate the crucial change in the electronic structure due to M-point frozen phonon S1 in-plane motion, we show in Fig. 6 the band structures of distorted and undistorted structures in the vicinity of the Fermi level. The black lines depict the undistorted energy bands while the red lines correspond to the frozen-phonon distorted structure with S1 displacement by 0.18 Å. For comparison, both lines are drawn in a $\sqrt{2} \times \sqrt{2} \times 1$ supercell. A considerable difference in band structures induced by the in-plane S1 displacement indicates a large electron-phonon coupling from this CDW instability.

The depth of the double well is only about 100 cm^{-1} indicates that the displacements of S atom are probably

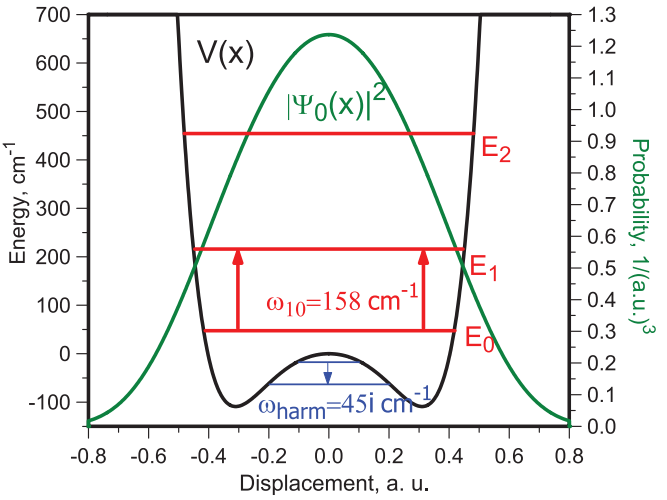

FIG. 5. (Color online) Calculated double-well potential for the unstable phonon mode using the frozen phonon method. The probability plot of the ground state atomic wave function and the first three eigenvalues of the anharmonic model are also shown.

dynamic. We therefore extend the equilibrium position analysis by solving numerically Schrodinger's equation for the anharmonic potential well found from frozen phonon calculations, as shown in the black line of Fig. 5. The so obtained ground state atomic wave function is indeed centered at the high symmetry position, as demonstrated by the probability curve shown in green line of Fig. 5. It is therefore clear that the above mentioned unstable modes are not related to a statically distorted structure of $LaO_{0.5}F_{0.5}BiS_2$. This is consistent with experimental observations that the resistivity changes smoothly from 300 K to about 10 K where the superconductivity occurs.[8,12]

We then turn our discussion to the wave-vector (**q**) and mode (ν) -dependent electron-phonon coupling $\lambda_\nu(\mathbf{q})$. At first, this can be done for all stable phonons. Calculation shows that the O/F modes have a negligible contribution to electron-phonon coupling. With strong hybridization, the coupling, however, is relatively strong for the BiS-based modes. For example, we can find λ's of the order of 1 for the S2-based

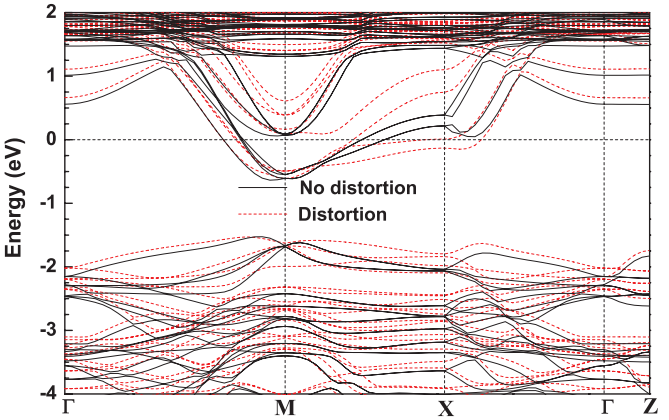

FIG. 6. (Color online) Calculated band structure. Black lines are the undistorted bands, red lines are the distorted bands corresponding to the S1 in-plane displacement. See text for details.

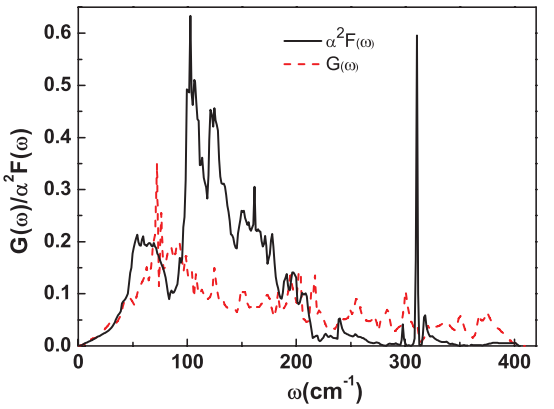

FIG. 7. (Color online) Calculated phonon density of states $G(\omega)$ and electron-phonon spectral function $\alpha^2F(\omega)$ for $La(O_{0.5}F_{0.5})BiS_2$.

optical phonons around 310 cm^{-1} near the Γ point. The analysis of the polarization vectors shows that these vibrations involve S2 movements toward Bi atoms. Unfortunately, finding the integral value of λ is a challenging problem due to the appearance of the imaginary frequencies, although neglecting completely the unstable modes results in already large average coupling constant (0.75) calculated using a $4 \times 4 \times 2$ q mesh. This is mainly due to the discussed S1/S2 vibrations.

To find the contribution for the four anharmonic modes, we follow the strategy of Ref. 22, where transitions from the ground to all phonon excited states of the anharmonic well need to be taken into account. The detailed theory using the total energy frozen phonon method has been elaborated in Ref. 23. Our numerical value of λ for the four anharmonic modes at the M point is 0.4. It has to be weighted somewhat by the area of the Brillouin zone where the actual instability

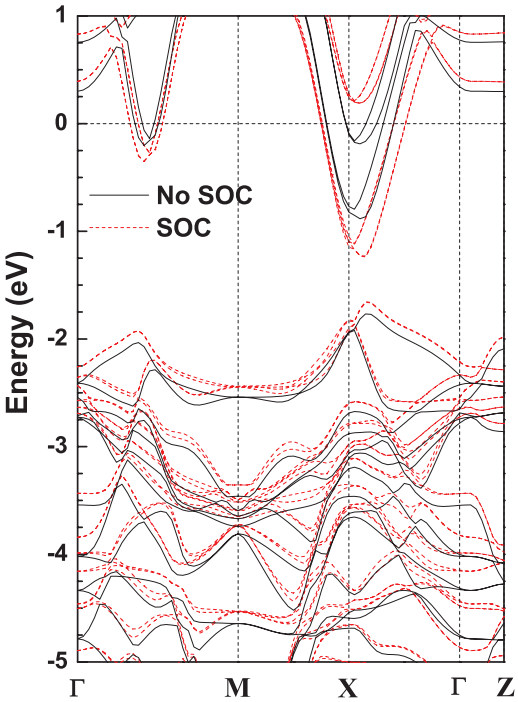

FIG. 8. (Color online) Band-structure plot with SOC of $La(O_{0.5}F_{0.5})BiS_2$.

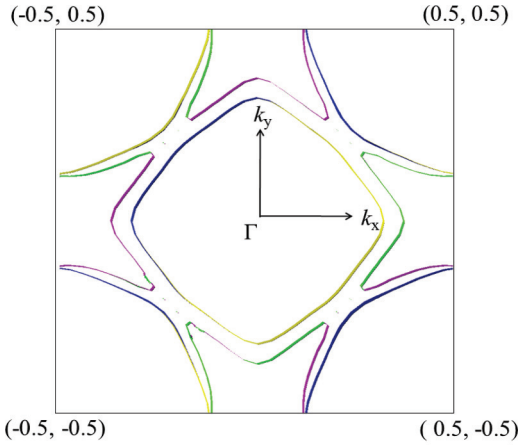

(a)

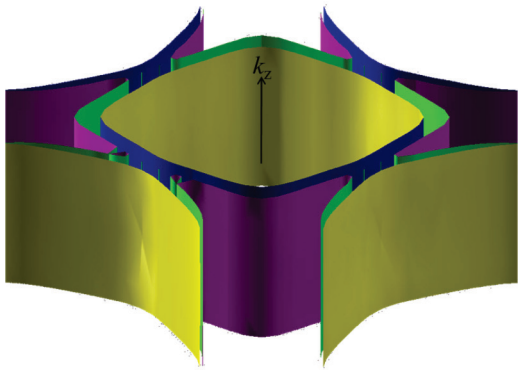

(b)

FIG. 9. (Color online) SOC results of the Fermi surface of $La(O_{0.5}F_{0.5})BiS_2$ (a) cross section for $k_z = 0$ and (b) 3D view.

occurs, therefore adding it to the result for harmonic λ should give us a total coupling constant of 0.85. Inserting this value into the McMillan formula for T_c, with the Coulomb parameter $\mu^* \simeq 0.1$ and $\omega_D = 260$ K, yields values of $T_c \simeq 11.3$ K in reasonable agreement with experiment. The obtained Eliashberg spectral function using stable phonon modes, together with the calculated phonon density of states, is shown in Fig. 7, which indicates the strong electron-phonon interaction in $La(O_{0.5}F_{0.5})BiS_2$.

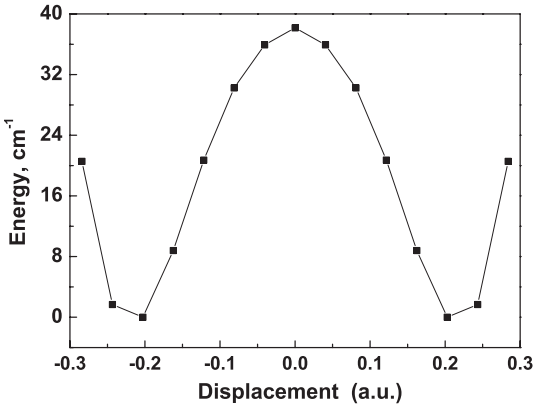

FIG. 10. Double-well potential for the unstable phonon mode using the frozen phonon method from the calculation with SOC.

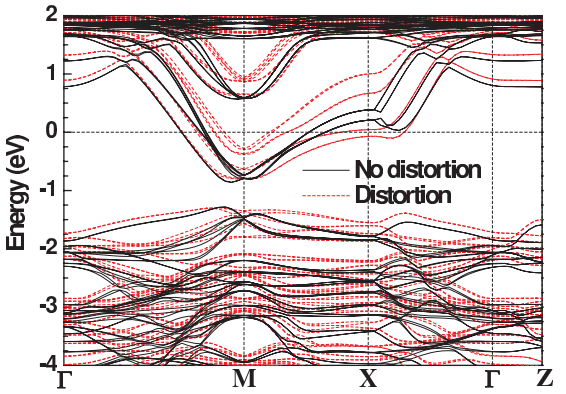

FIG. 11. (Color online) Band structure from calculation with SOC. Black lines are the undistorted bands, red lines are distorted bands corresponding to the S1 in-plane displacement.

Finally, to study the influence of SOC, we have also performed the calculation including SOC. We find that the optimized lattice parameters and Wyckoff positions of $La(O_{0.5}F_{0.5})BiS_2$ are similar with those without SOC calculation.

We show the band structure with and without the SOC in Fig. 8. As can be seen from Fig. 8, the SOC has a considerable effect on the bands around the X point. To be specific, there are four bands crossing the Fermi level in the band structure without SOC, whereas including SOC pushes two bands above the Fermi level. Nevertheless, it is very interesting to notice that the Fermi surface from SOC calculation is still quite similar to that without SOC (see Fig. 3). As shown in Fig. 9, including SOC does not change the two-dimensional-like feature of the Fermi surface. Moreover, the strong Fermi surface nesting can still be found at wave vectors near $\mathbf{k} = (\pi,\pi,0)$, as shown in Fig. 9(a), and the main effect of SOC is to eliminate a small pocket around the X point.

To check the effect of SOC on the CDW instability, we also perform four SOC calculations by moving the atoms according to the eigenvectors of the four unstable phonon modes at the M point. Our frozen phonon calculations show that the double-well potential remains, though the well-depth drops considerably, as shown in Fig. 10.

We show in Fig. 11 the band structures of distorted and undistorted structures due to M-point frozen phonon S1

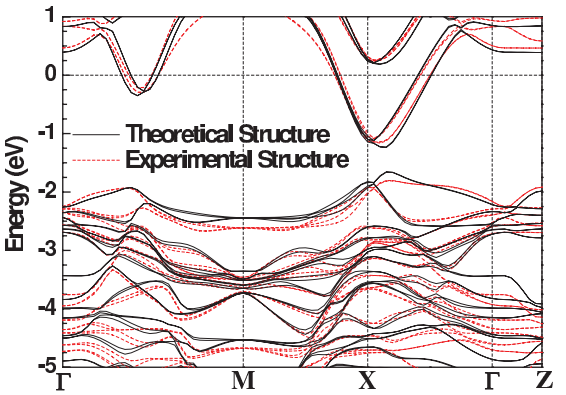

FIG. 12. (Color online) Band structure from the calculation with SOC.

in-plane motion in the vicinity of the Fermi level. As with the calculation without SOC, there is a considerable difference in band structures induced by the in-plane S1 displacement, which again indicates a large electron-phonon coupling from this CDW instability. The large electron-phonon coupling can also be found from a comparison of the band structure with the theoretical structure and the experimental structure, as shown in Fig. 12.

As a final comment, we recall that the calculation without SOC is found for heavy element Pb to be satisfactory,[24] therefore we do not foresee significant changes in our estimation of the electron-phonon interaction when the SOC effect is taken into account.

IV. CONCLUSIONS

In conclusion, the electronic structure, lattice dynamics, and electron-phonon interaction of the newly found superconductor $LaO_{0.5}F_{0.5}BiS_2$ have been investigated using density-functional theory and the linear-response approach. A strong Fermi surface nesting at $(\pi,\pi,0)$ results in large phonon softening and strongly anharmonic double-well behavior of the total energy as a function of the in-plane S displacements. A large electron-phonon coupling constant $\lambda = 0.85$ is predicted, which emphasizes that $LaO_{0.5}F_{0.5}BiS_2$ is a strongly coupled electron-phonon superconductor.

ACKNOWLEDGMENTS

X.G.W acknowledges useful conversations with H. H. Wen, J. X. Li, and Q. H. Wang. The work was supported by the National Key Project for Basic Research of China (Grants No. 2011CB922101 and No. 2010CB923404), NSFC under Grants No. 91122035, No. 11174124, No. 10974082, No. 61125403, and No. 50832003), PAPD, PCSIRT, and NCET. Computations were performed at the ECNU computing center. S.Y.S. was supported by DOE Computational Material Science Network (CMSN) Grant No. DESC0005468.

[1] W. E. Pickett, Rev. Mod. Phys. **61**, 433 (1989).
[2] Y. Maeno, H. Hashimoto, K. Yoshida, S. Nishizaki, T. Fujita, J. G. Bednorz, and F. Lichtenberg, Nature (London) **372**, 532 (1994).
[3] J. Nagamatsu, N. Nakagawa, T. Muranaka, Y. Zenitani, and J. Akimitsu, Nature (London) **410**, 63 (2001).
[4] Y. Kamihara, T. Watanabe, M. Hirano, and H. Hosono, J. Am. Chem. Soc. **130**, 3296 (2008).
[5] J. Paglione and R. L. Greene, Nat. Phys. **6**, 645 (2010).
[6] J. Dong, H. J. Zhang, G. Xu, Z. Li, G. Li, W. Z. Hu, D. Wu, G. F. Chen, X. Dai, J. L. Luo, Z. Fang, and N. L. Wang, Europhys. Lett. **83**, 27006 (2008).
[7] Y. Mizuguchi, H. Fujihisa, Y. Gotoh, K. Suzuki, H. Usui, K. Kuroki, S. Demura, Y. Takano, H. Izawa, and O. Miura, Phys. Rev. B **86**, 220510(R) (2012).
[8] Y. Mizuguchi, S. Demura, K. Deguchi, Y. Takano, H. Fujihisa, Y. Gotoh, H. Izawa, and O. Miura, J. Phys. Soc. Jpn. **81**, 114725 (2012).
[9] S. Demura, Y. Mizuguchi, K. Deguchi, H. Okazaki, H. Hara, T. Watanabe, S. J. Denholme, M. Fujioka, T. Ozaki, H. Fujihisa, Y. Gotoh, O. Miura, T. Yamaguchi, H. Takeya, and Y. Takano, arXiv:1207.5248.
[10] S. Li, H. Yang, J. Tao, X. Ding, and H. H. Wen, arXiv:1207.4955; J. Xing, S. Li, X. Ding, H. Yang, and H.-H. Wen, Phys. Rev. B **86**, 214518 (2012).
[11] S. G. Tan, L. J. Li, Y. Liu, P. Tong, B. C. Zhao, W. J. Lu, and Y. P. Sun, Physica C **483**, 94 (2012).
[12] H. Kotegawa, Y. Tomita, H. Tou, H. Izawa, Y. Mizuguchi, O. Miura, S. Demura, K. Deguchi, and Y. Takano, J. Phys. Soc. Jpn. **81**, 103702 (2012).
[13] H. Usui, K. Suzuki, and K. Kuroki, Phys. Rev. B **86**, 220501 (2012).
[14] T. Zhou and Z. D. Wang, arXiv:1208.1101.
[15] V. P. S. Awana, A. Kumar, R. Jha, S. Kumar, J. Kumar, A. Pal, Shruti, J. Saha, and S. Patnaik, Solid State Commun. **157**, 21 (2013).
[16] S. K. Singh, A. Kumar, B. Gahtori, G. Sharma, S. Patnaik, and V. P. S. Awana, J. Am. Chem. Soc. **134**, 16504 (2012).
[17] J. P. Perdew, K. Burke, and M. Ernzerhof, Phys. Rev. Lett. **77**, 3865 (1996).
[18] G. Kresse and J. Furthmuller, Comput. Mater. Sci. **6**, 15 (1996); Phys. Rev. B **54**, 11169 (1996).
[19] P. Giannozzi *et al.*, J. Phys.: Condens. Matter **21**, 395502 (2009).
[20] S. Baroni, S. de Gironcoli, A. Dal Corso, and P. Giannozzi, Rev. Mod. Phys. **73**, 515 (2001).
[21] Z. P. Yin, S. Lebegue, M. J. Han, B. P. Neal, S. Y. Savrasov, and W. E. Pickett, Phys. Rev. Lett. **101**, 047001 (2008).
[22] J. C. K. Hui and P. B. Allen, J. Phys. F **4**, L42 (1974).
[23] V. Meregalli and S. Y. Savrasov, Phys. Rev. B **57**, 14453 (1998).
[24] S. Y. Savrasov and D. Y. Savrasov, Phys. Rev. B **54**, 16487 (1996).